Proceedings of the 9th U.S. National and 10th Canadian Conference on Earthquake Engineering
Compte Rendu de la 9ième Conférence Nationale Américaine et
10ième Conférence Canadienne de Génie Parasismique
July 25-29, 2010, Toronto, Ontario, Canada • Paper No 1108

ADVANCED IMPLEMENTATION OF NONLINEAR CONTROL ALGORITHMS FOR SHAKING TABLE TESTS

T.Y. Yang[1] and A. Schellenberg[2]

ABSTRACT

The shaking table testing method is one of the main experimental techniques to evaluate the dynamic response of structural systems under earthquake loads. This experimental method produces nearly realistic prototype conditions, giving important insight into critical issues such as collapse mechanisms, component failures, acceleration amplifications, residual displacements and post-earthquake capacities. Traditionally shaking table control systems have been tuned using linear controllers, which are designed to regulate linear systems. With most of the specimens being tested to highly nonlinear states (to understand the structural response under extreme loading conditions), linear controllers can no longer control the shaking table effectively. This leads to experimental errors between commanded and measured table movements, which may produce an unintended response of the tested structure. Ultimately, it may even result in a pre-mature failure of the specimen. A nonlinear control algorithm, based on the Lyapunov stability theorem, is utilized to control a shaking table test of a nonlinear single-degree-of-freedom system with the goal to account for the nonlinear response of the specimen, model uncertainties and other disturbances affecting the experiment test. Simulation results indicate that the investigated nonlinear control algorithm can be used to achieve excellent tracking, even when the tested structure behaves nonlinearly. The example also demonstrates the ability of the nonlinear control algorithm to compensate for disturbances, where the actuator force input to the shaking table plant is altered with respect to the force command that the control algorithm puts out. Thus, the proposed nonlinear shaking table control algorithm is not only a viable alternative to more traditional controllers, but also a way to significantly improve the quality of shaking table tests.

Introduction

Traditional control of shaking table tests is based on the use of linear control algorithms (such as PID controllers), to minimizing tracking errors between the command and feedback signals. However due to the nonlinear nature of most tested specimens, it is very difficult, or impossible, to achieve excellent tracking using such linear control algorithms. Thus, a nonlinear control algorithm, the sliding mode control (SMC) strategy, is chosen to regulate the movement of the shaking table (Slotine and Li, 1991). The sliding mode controller is designed using a Lyapunov-like stability function, which permits the algorithm to control nonlinear systems. In addition, the sliding mode controller contains an inherent robustness term, which is capable of compensating for any model uncertainties. This is especially useful in the environment of experimental testing, where most of the model parameters are not easily assessable. In this paper,

[1] Assistant Professor, Dept. of Civil Engineering, University of British Columbia, Vancouver, BC, Canada.
[2] Post Doctoral Scholar, Dept. of Civil and Env. Engineering, University of California, Berkeley, CA, USA.

a sliding mode control algorithm is derived to regulate a unidirectional shaking table, where a nonlinear single-degree-of-freedom specimen is tested. Similar approaches could be utilized for multi-degree-of-freedom systems tested on multidirectional shaking tables. To evaluate the performance and accuracy of the developed sliding mode controller, the response of the shaking table and the single-degree-of-freedom bridge column specimen are compared against the open-loop (OL) and the traditional PID control algorithms.

Modeling of the system

Fig. 1 shows the model of a cantilever bridge column that is being tested on a unidirectional shaking table. For modeling purposes the column is idealized as a single-degree-of-freedom specimen. Hence, the only two free degrees-of-freedom of the system are d_t and d_s, which represent the absolute displacement of the shaking table and the relative displacement of the specimen, respectively.

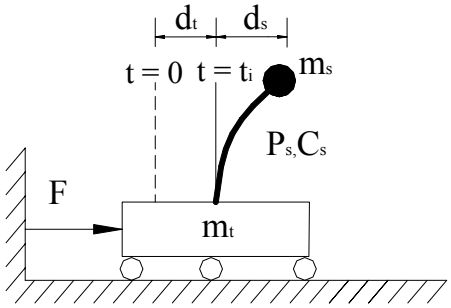

Figure 1: Model of the idealized system.

To simulate the seismic response of the simplified model shown above, parameters from the shaking table tests conducted by Mahin et al. (2006) are adopted for this study. The tested specimen had an unbonded post-tensioning tendon in the center of the column, which provided a restoring force to re-center the specimen after severe earthquake shaking. To simplify the modeling assumptions, the flag-shaped hysteresis-loop of the specimen was replaced by a hysteresis-loop without re-centering capability. The adopted hysteresis-loop represents a column with similar initial stiffness and strength but without the stiffness degradation after cycles of inelastic deformation. Figs. 2a and 2b show the picture of the prototype model, the displacement loading history and the corresponding hysteresis-loops of the idealized cantilever column specimen.

The dynamic response of the shaking table and specimen configuration shown in Fig. 1 can be modeled using the two 2nd-order nonlinear differential equations shown in Eq. 1.

$$\begin{aligned} m_s\left(\ddot{d}_t+\ddot{d}_s\right)+c_s\dot{d}_s+P_s\left(d_s,\dot{d}_s\right)&=0 \\ m_t\ddot{d}_t-c_s\dot{d}_s-P_s\left(d_s,\dot{d}_s\right)-F&=0 \end{aligned} \tag{1}$$

where $\dot{d}_t$, $\ddot{d}_t$, $\dot{d}_s$ and $\ddot{d}_s$ are the absolute velocity and acceleration of the table and the relative velocity and acceleration of the specimen, respectively. m_t is the mass of the shaking table, m_s

is the mass of the specimen, c_s is the damping of the specimen, P_s is the nonlinear resisting force of the specimen and F is the control force of the actuator. To model the nonlinear resisting force of the specimen, a Bouc-Wen model (Bouc 1971; Wen 1976) shown in Eq. 2 is used.

$$\begin{aligned} P_s\left(d_s,\dot{d}_s\right) &= \alpha\, k_{e,s}\, d_s + (1-\alpha) k_{e,s}\, d_{y,s}\, z \\ 0 &= d_{y,s}\,\dot{z} + \gamma\left|\dot{d}_s\right| z\left|z\right|^{n-1} + \beta\dot{d}_s\left|z\right|^n - \dot{d}_s \end{aligned} \tag{2}$$

where α is the ratio of the post-yield to elastic stiffness, $k_{e,s}$ is the elastic stiffness, $d_{y,s}$ is the yield displacement, z is a time varying hysteretic parameter which can be solved for using Eq. 2b and β, γ and n are dimensionless parameters that control the shape of the hysteresis-loops.

To solve the system of equations, the two 2nd-order differential equations (Eq. 1) are transformed into a state space representation as shown in Eq. 3. The dynamic response of the system is solved using the ode23s solver in MATLAB (MathWorks 2008). Values of 1e-6 were selected for both the relative and absolute tolerances.

$$\begin{Bmatrix} x_1 \\ x_2 \\ x_3 \\ x_4 \\ x_5 \end{Bmatrix} = \begin{Bmatrix} d_t \\ \dot{d}_t \\ d_s \\ \dot{d}_s \\ z \end{Bmatrix} \Rightarrow \begin{Bmatrix} \dot{x}_1 \\ \dot{x}_2 \\ \dot{x}_3 \\ \dot{x}_4 \\ \dot{x}_5 \end{Bmatrix} = \begin{Bmatrix} x_2 \\ \dfrac{1}{m_t}\left(P_s\left(x_3,x_5\right)+c_s x_4 + F\right) \\ x_4 \\ -\dfrac{1}{m_t}\left(P\left(x_3,x_5\right)_s + c_s x_4 + F\right) - \dfrac{1}{m_s}\left(P_s\left(x_3,x_5\right)+c_s x_4\right) \\ \dfrac{1}{d_{y,s}}\left(x_4 - \gamma\left|x_4\right| x_5\left|x_5\right|^{n-1} - \beta x_4\left|x_5\right|^n\right) \end{Bmatrix} \tag{3}$$

a) Picture of the prototype model on the EERC shaking table.

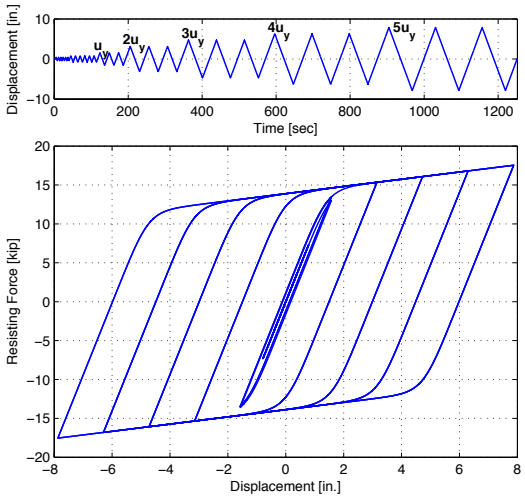

b) SAC loading history and hysteresis-loops of the idealized model.

Figure 2: Picture of the prototype model and the idealized force-deformation hysteresis-loops.

Selection of the ground motion and benchmark response

To compare the effectiveness of the different control algorithms, the seismic response of the idealized model was analyzed using the SACNF01 near-fault ground motion selected from the SAC ground motion database (Somerville 1997). The ground motion was originally recorded during the 1978 Tabas earthquake and amplitude scaled and baseline corrected to match the capacities of the EERC shaking table located at the University of California, Berkeley. Fig. 3 shows the time history records of the ground motion. The dynamic response of the specimen excited by the selected ground motion was simulated using a fixed-base excitation (Fig. 4) and used as the benchmark response to evaluate the effectiveness of the control algorithms.

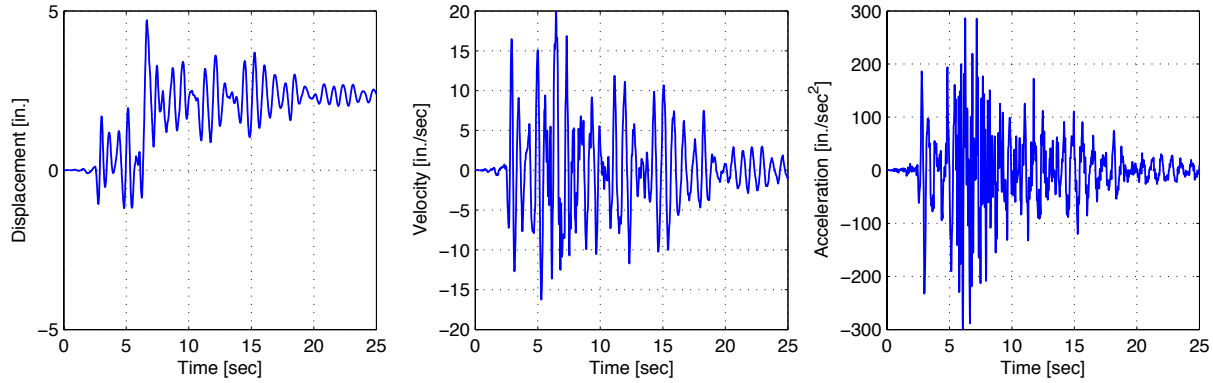

Figure 3: SACNF01 near-fault ground motion record.

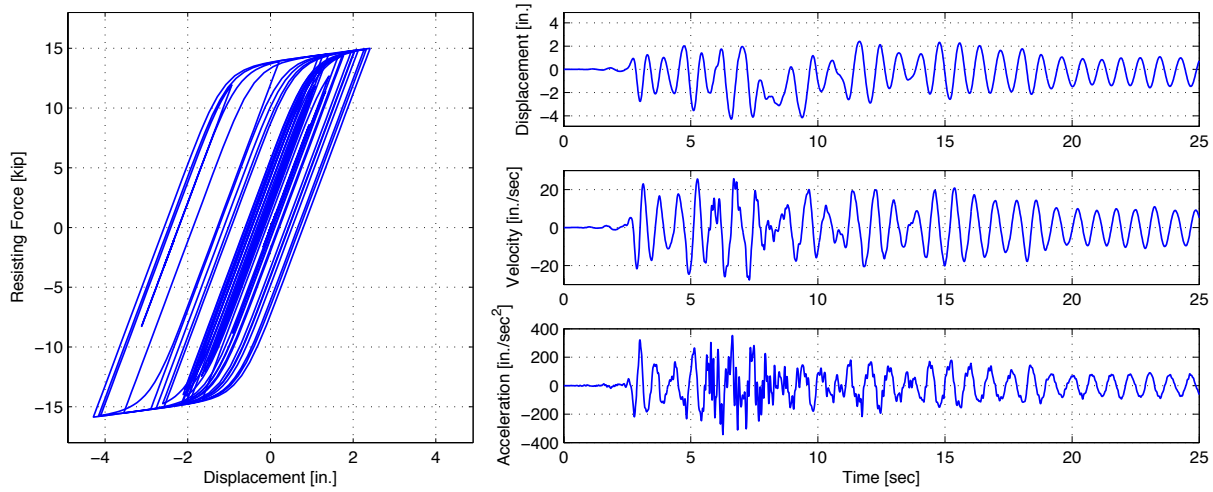

Figure 4: Response of the specimen subjected to the SACNF01 near-fault ground motion.

Selection and implementation of the control algorithms

Open-Loop Control (OL)

The simplest control algorithm to regulate the shaking table is to use open-loop control. The controller calculates the actuator force by multiplying the sum of the table and specimen masses with the input acceleration. This control algorithm ignores the nonlinear interaction force

between the specimen and the table and does not adjust its input using any feedback measurements.

PID Control (PID)

To improve the performance of the open-loop control system, a closed-loop control technique (PID controller) was used. The controller adjusts the input signal to the table based on a linear combination of the feedback error, the integral of the feedback error and the derivative of the feedback error. By selecting the appropriate gains that multiply these three terms, the PID controller modifies the closed-loop dynamics, which in term forces the error dynamics of the system to zero asymptotically. Once the error dynamics reaches zero perfect tracking is obtained. The closed-loop dynamics of the system (including the PID controller) was implemented using the MATLAB/Simulink environment (MathWorks 2008) shown in Fig. 5. The plant represents the system dynamics of both, the shaking table and the test specimen. The input to the plant is the control force and the outputs of the plant are the different states of the table and specimen. The error dynamics of the system was selected based on the error of the table displacement. To minimize such error dynamics, three constant gains that multiply the feedback error, the integration of the feedback error and the derivative of the feedback error were selected. For the purpose of tuning the PID controller, the specimen was replaced by a rigid block of equal mass. This means that the interaction forces between the table and the specimen were ignored. This is a common approach for tuning shaking tables without damaging specimens prior to testing. However, the tuning of the PID controller still required some engineering judgment and experience. Once the PID controller had been tuned to satisfaction, the rigid block was replaced by the specimen.

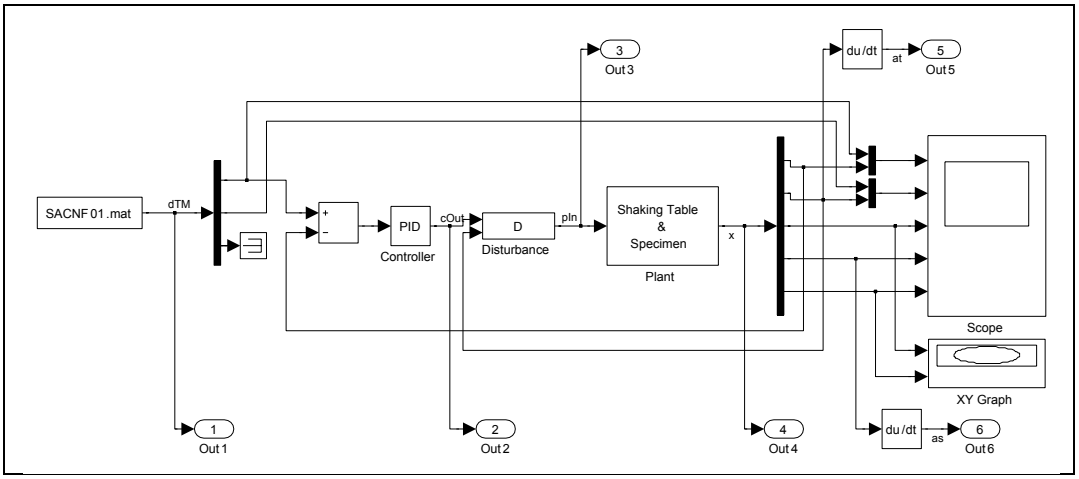

Figure 5: Simulink model of system with PID controller.

Sliding Mode Control (SMC)

The PID controller provides significant performance advantages over the open-loop controller. However, the performance of the PID controller is considerably affected by ignoring the nonlinear interaction force of the specimen and the influence of external disturbances. To overcome this disadvantage, a sliding mode control algorithm was used to regulate the shaking table instead.

Sliding mode control is one of the robust control techniques that aim at controlling nonlinear systems including model uncertainties and disturbances. The control algorithm employs a Lyapunov-like function to drive the tracking error towards zero asymptotically, which again provides the desired tracking. Even if there are model uncertainties and/or disturbances present, the sliding mode control algorithm is able to overcome these nonlinearities using its robustness term and achieve excellent tracking.

Design of the Sliding Mode Controller

The sliding mode controller is designed using a Lyapunov-like function such as the one shown in Eq. 4. Because Eq. 4a is a positive definite function, and if Eq. 4b is selected to be a negative definite function, the Lyapunov stability theorem guarantees that the scalar function, S, will go to zero asymptotically.

$$\begin{aligned} V &= \frac{1}{2}S^2 \\ \dot{V} &= S\dot{S} \end{aligned} \tag{4}$$

If S is defined as a combination of the displacement and velocity tracking error as shown in Eq. 5, and Eq. 4b is selected to be $-KS^2$ (a negative definite function), the Lyapunov stability theorem guarantees that S converges to zero asymptotically. This means that the solution $\tilde{x}_1 = e^{-\lambda t}$ of the tracking error equation will also converge to zero asymptotically and therefore achieve perfect tracking.

$$S = \dot{\tilde{x}}_1 - \lambda\tilde{x}_1 \tag{5}$$

where $\tilde{x}_1 = x_1 - x_{1d}$, $\dot{\tilde{x}}_1 = \dot{x}_1 - \dot{x}_{1d}$, λ is a strictly positive constant (that defines the exponential convergence rate on the sliding surface), x_1, $\dot{x}_1$ are the actual displacement and velocity of the table and x_{1d}, $\dot{x}_{1d}$ are the desired displacement and desired velocity of the table, respectively.

Taking the derivative of Eq. 5 and substituting the states from Eq. 3, the derivative of S can be expressed in terms of Eq. 6.

$$\dot{S} = \ddot{\tilde{x}}_1 - \lambda\dot{\tilde{x}}_1 = \frac{1}{m_t}\left(P_s + c_s x_4 + F\right) - \ddot{\tilde{x}}_{1d} + \lambda\left(x_2 - \dot{\tilde{x}}_{1d}\right) = CE\left(\tilde{x}\right) + \bar{f} + bF \tag{6}$$

where $CE\left(\tilde{x}\right) = \lambda\left(x_2 - \dot{\tilde{x}}_{1d}\right)$, $\bar{f} = \frac{1}{m_t}\left(P_s + c_s x_4\right) - \ddot{\tilde{x}}_{1d}$ and $b = \frac{1}{m_t}$.

Finally, substituting Eq. 6 and $\dot{V} = -KS^2$ into Eq. 4b, the following sliding mode control law is obtained.

$$\dot{S} = -KS \qquad \Rightarrow \qquad F = -\frac{1}{b}\left(CE\left(\tilde{x}\right) + \bar{f} + KS\right) \tag{7}$$

Evaluation of the control algorithms

To achieve a more realistic simulation of the system dynamics, an external disturbance and command saturation were added to the control force. For the purpose of this study, the control force was limited to 80% of the actuator capacity, which corresponded to 240 kips. The disturbance was modeled by adjusting the actuator forces utilizing a normal distributed random variable with mean of 1.0 and variance of 0.1.

Fig. 6 shows the tracking indicators for the table displacement, velocity and acceleration. The tracking indicators were calculated according to the formula presented in (Mercan and Ricles 2007). The indicator is based on the enclosed area of the hysteresis loops when actual output is plotted versus desired input. If the value of the indicator is increasing the response is leading. On the other hand, if the indicator is decreasing the response is lagging. The results show that the OL controller did not produce good tracking. The tracking indicator increases rapidly, leaving the graph after the first 2.5 seconds. On the other hand, the PID and SMC controllers were able to achieve good tracking. The SMC controller achieved the best tracking performance and in addition was not affected by the disturbance in any way. The PID controller performed slightly worse than the SMC controller. In addition, the tracking performance was clearly affected by the presence of the disturbance. These trends are even more pronounced for velocities and accelerations than for displacements.

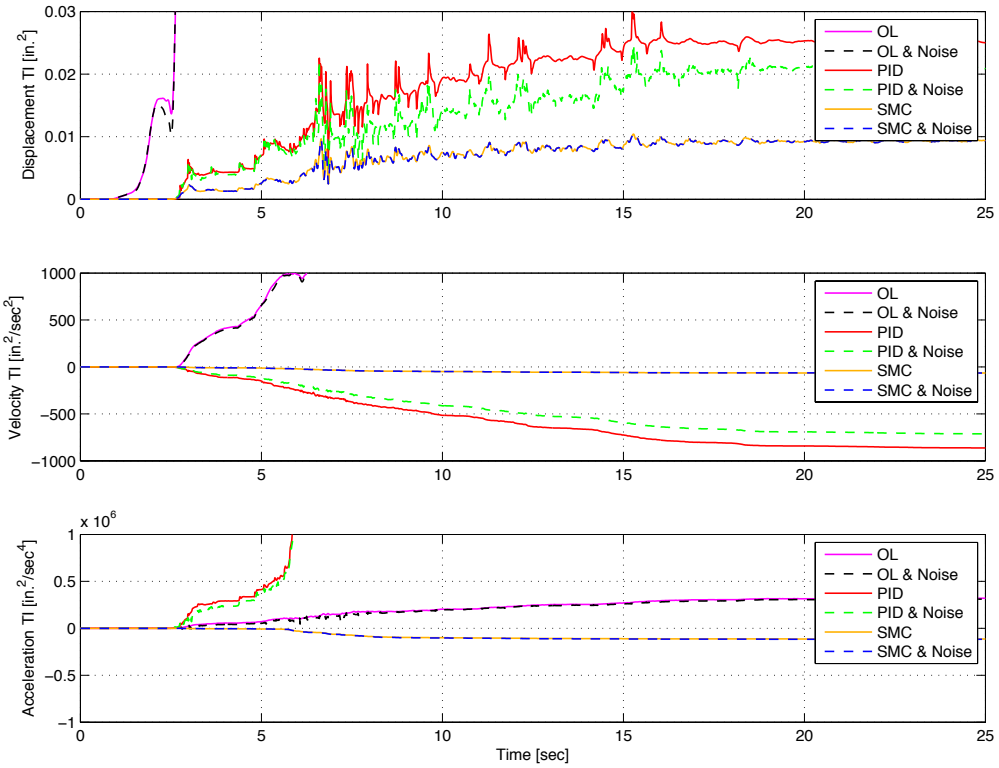

Figure 6: Tracking indicators of the table response for different control laws.

Table 1 shows the maximum control forces in the actuator. The results indicate that the PID controller requires the largest control force and reaches the saturation limited of the actuator. The SMC controller requires the least amount of control force. With the disturbance added to the

system, larger actuator forces are required.

Table 1. Maximum control forces in the actuator.

Control algorithm	Without disturbance	With disturbance
OL	133.7 kips	172.5 kips
PID	240.0 kips	240.0 kips
SMC	56.3 kips	167.8 kips

Fig. 7 illustrates the tracking indicators for the specimen response compared against the benchmark response presented in Fig. 4. The results indicate that the OL controller damages the specimen pre-maturely. The displacement tracking indicator increases out of bound. The PID and SMC controller both are able to achieve accurate displacement tracking. Similar trends are observed for the velocity tracking indicators. However, the acceleration tracking indicators demonstrate that the PID controller produces large acceleration errors, which is mainly caused by the saturation of the actuator force. On the other hand, the SMC controller produces excellent acceleration tracking. Similar structural responses are observed with and without the added disturbance.

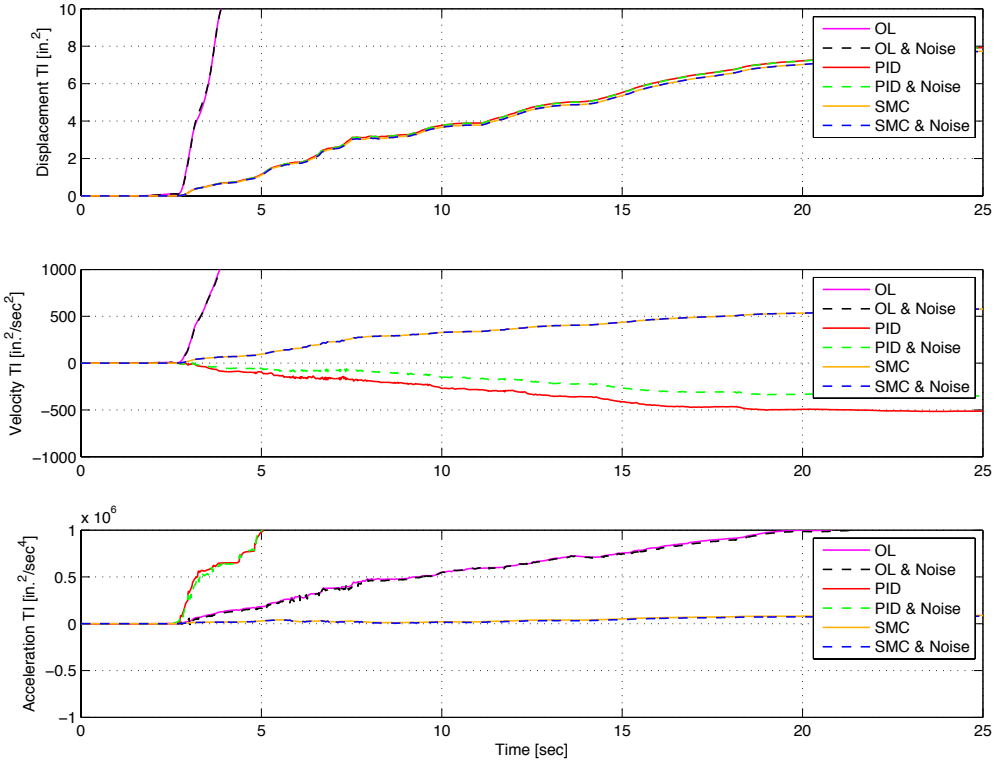

Figure 7: Tracking indicators of the specimen response for different control laws.

Robustness of the SMC

As shown in Eq. 7, the calculation of the control force for the SMC requires an estimate of model parameters such as the mass of the table, the mass of the specimen, the nonlinear resisting force of the specimen and the damping force of the specimen. These might be difficult

to measure during an experimental test. To demonstrate that the SMC is able to compensate for model uncertainties through its robustness term, the damping and nonlinear resisting forces of the specimen were over estimated by 20% and the mass of the table was underestimated by 20%. The results of the specimen response compared against the benchmark fixed-based response are presented in Fig. 8. The results show that the specimen response using the SMC controller matched almost perfectly with the benchmark response. This reconfirms the robustness of the SMC to regulate shaking table tests, especially when the specimen parameters are difficult to estimate prior to the execution of an experimental test.

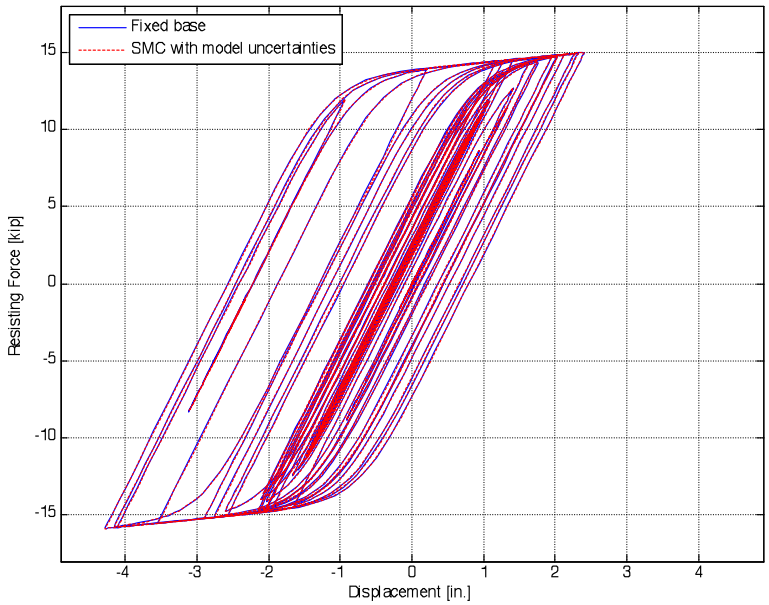

Figure 8: Comparison of the specimen response using fixed based excitation and SMC with model uncertainties.

Conclusions

The shaking table testing method is one of the most realistic experimental testing techniques to evaluate the dynamic response of structural systems. However, the accuracy of the shaking table test depends strongly on the control algorithm used to regulate the shaking table. In this paper, an idealized nonlinear single-degree-of-freedom system tested on a unidirectional shaking table has been studied. To properly model the system dynamics, the nonlinearity of the specimen, the saturation of the actuator control force and an additional external disturbance have been considered. Three different controllers were designed and implemented. The responses of the table and the specimen were then simulated for the different controllers with and without disturbances. As expected, the results indicated that the OL controller produced poor tracking in all situations. On the other hand, the PID controller was able to produce good displacement tracking, but performed poorly in tracking velocities and accelerations. Contrary, the SMC controller achieved excellent tracking for all response quantities. Furthermore, performance of the SMC was not affected by external disturbances and model uncertainties. This reconfirms the robustness of the SMC controller, making it a viable alternative for regulating experimental shaking table tests.

In addition, the SMC controller was able to achieve excellent tracking of the table movement with lower actuator forces, which ensured that the specimen was tested with the exact ground motion input. This provides a significant advantage over the traditional PID controller and allows for a larger range of specimens and configurations to be tested using the shaking table technique.

Further research should be conducted on the sliding mode control algorithm. Specifically, the performance of the controller should be verified in a real application in the laboratory environment. Also, the theory should be extended to multi-degree-of-freedom systems tested on multidirectional shaking tables. Once the implementation of the sliding mode controller has been validated experimentally, these research results can significantly contribute to the improvement of shaking table testing worldwide.

References

Bouc, R. 1971. Mathematical model for hysteresis. Report to the Centre de Recherches Physiques, pp16-25, Marseille, France.

Hedrick, J. K. 2004. Control of Nonlinear Dynamic Systems, ME237 class notes, Spring 2004. University of California, Berkeley, CA, United States.

Khalil, H. 2002. Nonlinear Systems, 3rd edition. Prentice-Hall, NJ, United States.

Mahin S. A., Sakai J. and Jeong H. 2006. Use of Partially Prestressed Reinforced Concrete Columns to Reduce Post-Earthquake Residual Displacements of Bridges. Proceedings of Fifth National Seismic Conference on Bridges & Highways, September 18-20, San Francisco, CA, United States.

MathWorks 2008. MATLAB and Simulink for Technical Computing. The MathWorks Inc., Natick, MA, United States.

Mercan, O. and Ricles, J. M. 2007. Stability and accuracy analysis of outer loop dynamics in real-time pseudodynamic testing of SDOF systems. *Earthquake Engineering and Structural Dynamics*, **36(11)**, 1523-1543.

Slotine, J. E. and Li W. 1991. Applied Nonlinear Control. Prentice-Hall, NJ, United States.

Somerville, P. et al. 1997. Development of Ground Motion Time Histories for Phase 2 of the FEMA/SAC Steel Project. Report SAC/BD-97/04, SAC Steel Project, Sacramento, CA, United States.

Wen, Y. K. 1976. Method for random vibration of hysteretic systems. *Journal of Engineering Mechanics Division*, **102(EM2)**, 249–263.